American Journal of Bioscience and Clinical Integrity
https://biojournals.us/index.php/AJBCI
ISSN: 2997-7347

Article

Fabrication of PANI/ $NiCo_2O_4$ /CeO_2 Nanocomposite: Preparation and Characterization

Ammar Adil Hussein[1, 2, 3]*, Ali M. A. Abdul Amir AL-Mokaram[1]*, Qabas Naji Rashid[2]
[1] Department of Chemistry, College of Science, Mustansiriyah University, Baghdad, 10052, Iraq
[2] Department of Chemistry, College of Pharmacy, Tikrit University, Tikrit, Iraq
[3] Department of Chemistry, Baghdad College High School, Ministry of Education, Iraq
Correspondence: amaradel61@gmail.com, ali75@uomustansiriyah.edu.iq*, qabas.naji@tu.edu.iq

Citation: Hussein, A. A., AL-Mokaram, A. M. A. A., & Rashid, Q. N. Fabrication of PANI/ $NiCo_2O_4$ /CeO_2 Nanocomposite: Preparation and Characterization. American Journal of Bioscience and Clinical Integrity 2024, 1(9), 39-47.

Received: 28th Aug 2024
Revised: 4th Sept 2024
Accepted: 10th Sept 2024
Published: 18th Sept 2024

Abstract: This study introduces innovative research on synthesizing pure polyaniline (PANI) and a binary nanocomposite via in situ chemical oxidation polymerization. A modified interfacial polymerization technique was used to produce a greenish-black PANI/$NiCo_2O_4$/CeO_2 nanocomposite. Characterization methods such as Fourier transform infrared spectroscopy (FT-IR), UV-visible spectroscopy, and powder X-ray diffraction (XRD) were applied to the nanocomposite. The nanoscale structure of the composite was confirmed through particle size analysis in Field Emission Scanning Electron Microscopy (FE-SEM) images, which showed a uniform PANI coating on the $NiCo_2O_4$/CeO_2 nanocomposite. Infrared spectroscopy identified all the characteristic vibrational bands of polyaniline and additional bands from the spinel metal oxides. XRD analysis verified the presence of $NiCo_2O_4$/CeO_2, with broader peaks representing polyaniline and sharper peaks indicating the metal oxides.

Keywords: polyaniline, nickel cobalt oxide, cerium oxide, nanocomposite, X-ray diffraction (XRD)

Introduction

Nanotechnology has contributed significantly to developing new classes of materials with enhanced functionality and applications. The scientific definition of nanocomposite is multiphase materials where one or several phases have at least one dimension less than 100 nm. Since the introduction of nanotechnology, the focus has been directed towards designing and developing efficient immobilizing nanostructures to achieve desired outcomes [1].

As a result of its environmental stability and electrical and electrochemical characteristics, Polyaniline, known as PANI, has received enormous attention and has been the focus of many studies conducted on polymers to improve some of its properties. It is also up to be hybridized with some nanocomposites [2]. Metal oxide nanoparticles serve as a significant doping agent for modifying the characteristics of polymer chains [3]. The doping process that occurs through the oxidation of nitrogen atoms of polyaniline chain rings by cation and radical cations through the conducting polymer with inorganic nanoparticle composites in different combinations for two components has been under considerable consideration and interest [4]. Due to their interesting physical and electro-conductive properties, electronically conducting polymers, like polypyrrole, polyaniline, polythiophene etc. have been the focus of many researchers in the scientific community [5]. Conducting polymer composite can be fabricated from an aqueous solution of monomer and insulating polymer in different methods such as chemical or electrochemical polymerization by using suitable dopants and oxidants or supporting electrolytes [6, 7]. Scientific researchers have been recording and exploring the deposition of nanoscale PANI into numerous pores of $NiCo_2O_4$ nanorod arrays. The referred-to method modifies the integrity of the electrode by enabling the porous support to better accommodate the strain and stabilize PANI [8, 9, 10]. This research work contributes to the synthesis of pure polyaniline and binary nanocomposite by situ chemical oxidation polymerization and fabricated a novel PANI/$NiCo_2O_4$ nanocomposite /CeO_2.

Materials and Methods

Ammonium persulfate (APS), H_2SO_4, $NiCl_2.6H_2O$, $CoCl_2.6H_2O$ and aniline were obtained from Merck and Sigma-Aldrich, India. CeO_2 nanoparticles were purchased from Hongwu new material from China. Samples have been investigated by JASCO FT-IR- 4200 analysis and PerkinElmer UV/Vis spectroscopy in the polymer research unit library of the Science College of Al-Mustansiriyah University. A Raman shift was recorded with a TEKSAN N1–541 instruments in Hungary. Nanocomposites are examined and placed on a glass substrate for X-ray diffraction analysis, a device that was used is XRD- 6000 Shimadzu and FE-SEM images have been investigated by TESCAN Mira3 in Iran.

2.1. Preparation PANI/$NiCo_2O_4$/CeO_2 nanocomposites

PANI/$NiCo_2O_4$/CeO_2 nanocomposite is the resultant of the oxidation process of aniline with ammonium persulfate (APS) in aqueous solution. Likewise, 1 ml of aniline is diluted with 55 ml of H_2SO_4 (0.5 M) and stirred well in a cooling bath [11, 12]. Nano powder of $NiCo_2O_4$ and CeO_2 (15wt %) with an equal amount of each is mixed with the previously prepared solution in an ultrasonic device. After being sonicated for 1 hour, the colour of the mixture starts to change based on the amount of $NiCo_2O_4$ and CeO_2 [13, 14]. Then the resultant mixture is taken out of the ultrasonic device and brought to a magmatic stirrer for 1 hour. 50 ml of the cold solution, the oxidizing agent of APS (0.1 M), is carefully added to the mixture with continuous stirring for more than 2 hours. After the stirring, the reaction is left for about 4 hours at 0 to 5°C. The product of the reaction obtained from filtration was gathered and washed thoroughly with acetone and distilled water till the filtrate lost its colour. When it gets colourless, the filtrate is left at 80°C for 24 hours to dry [15, 16].

Results and Discussion

The FTIR spectra of PANI and PANI/ CeO_2 are respectively demonstrated in the (1-A) and (1-B) figures. Near 3224 cm^{-1}, the N–H stretching vibration reaches its highest value of PANI. The peck of 1556 cm^{-1} for C=N of quinone ring as well the peck of 1481 cm-1 for C=C of benzene ring in PANI. The distinguish peak 1285 cm^{-1} of the stretching vibration of secondary amine C–N associated with ring and C=C of quinone ring observed at 943 - 1230 cm^{-1} for the absorption peak. Almost near the peak at 1008 cm^{-1} shows the stretching vibration peak of C–H for PAINI absorption [17-20]. The FTIR spectra of PANI/ CeO_2 between (490 to 3224) are presented in Figure (1-B). Around peaks 3224 cm^{-1},1561 and 1481 cm^{-1}, were observed for N–H, C=N and C=C in PANI respectively. The peaks at 1295 cm^{-1}, and 927 - 1230 cm-1 indicate C–N and for quinone of C=C individually. In PANI, the absorption value nearby 1024 cm^{-1} for stretching vibration peak of C–H. In the main stretching vibration peak of CeO_2, the absorption reaches its highest value around 490, 540,693 cm^{-1} [21-25].

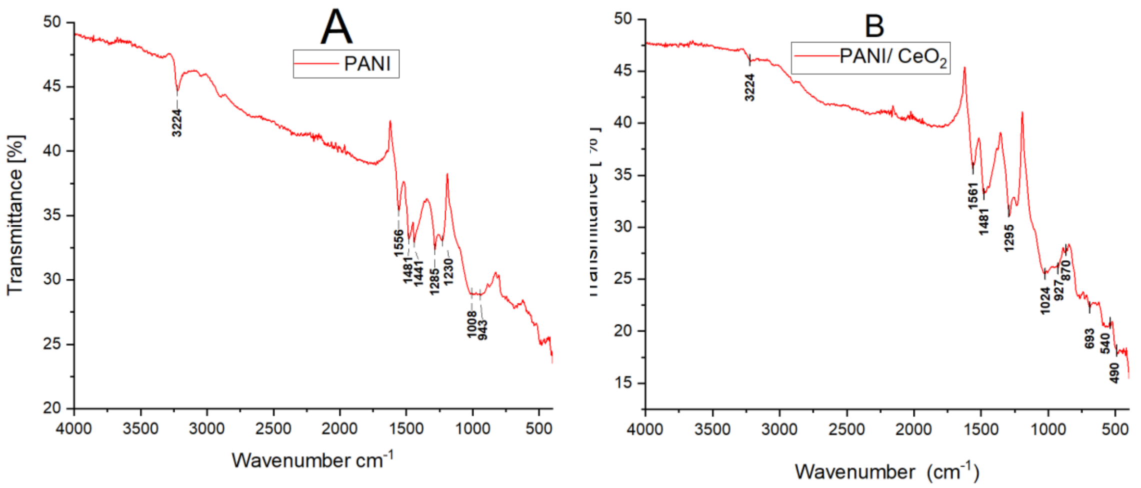

Figure 1. A- The FTIR spectra of PANI and B- the FTIR spectra of PANI/ CeO_2nanocomposite

Figure (2-A) and (2-B) respectively demonstrate the FT-IR spectrum of the PANI /$NiCo_2O_4$ and PANI/$NiCo_2O_4$ /CeO_2. In Figure (2-A), the acute peaks of the electro-active material at 540 and 640 cm^{-1} could be a result of the Ni-O and Co-O stretching vibrations and formation of the spinel $NiCo_2O_4$ nanostructure of the FTIR spectra with PANI. The N–H stretching vibration value reaches its highest in PANI around 3224 cm^{-1}. The values of C=N for quinone, C=C for benzene ring and C–N confirmed around 1556 cm^{-1}, 1450 cm^{-1} and 1285 respectively. Additionally, the C=C of the quinone ring is at 870 - 1230 cm^{-1}. The peak is at 1020 cm^{-1}, for PANI approval. The Ni-O and Co-O stretching vibrations and formation of the spinel $NiCo_2O_4$ nanostructure cause the acute peaks at 540 and 640 cm^{-1} [26, 27]. On the other hand, figure (2-B) presents the N–H, C=N for quinone, and C=C for benzene ring at 3224 cm^{-1}, 1556 cm^{-1} and 1481 cm^{-1} respectively. The characteristic peak of 1285 cm^{-1} is related to C–N associated with the ring, whereas the absorption peak of 945-1230 cm^{-1} relates to the C=C of the quinone ring. The high-value peak of stretching vibration of C–H is the nearby 1050 cm^{-1} in PANI. The acute peaks at 540 and 640 cm^{-1} are linked to the Ni-O and Co-O stretching vibrations and formation of the spinel $NiCo_2O_4$ nanostructure. The absorption reaches its highest value around 490, 540, and 693 cm^{-1} in the main stretching vibration peak of CeO_2.

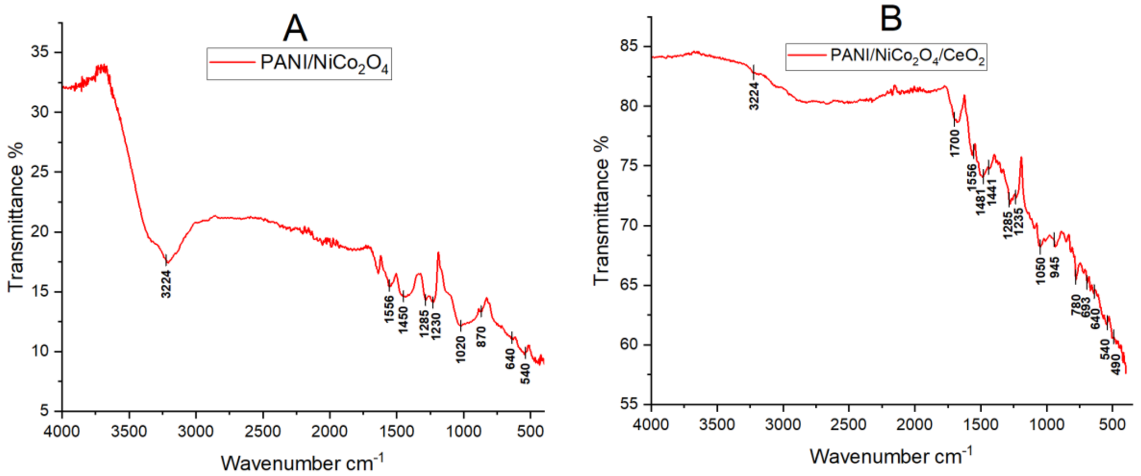

Figure 2. A- The FTIR spectra of PANI /$NiCo_2O_4$ and B -PANI/$NiCo_2O_4$/CeO_2 nanocomposite

The study of UV-visible absorption spectra can contribute to the understanding of the electronic structure of the optical band gap of the material. The absorption that occurs close to the ultraviolet region results from electronic transitions associated with the prepared sample. The PANI spectrum containing two distinguished peaks at 333 nm and 635 nm can be observed by UV–visible absorption spectra of pure PANI nanoparticles in Figure (3). The nanocomposite is found to be in an emeraldine state with absorbance peak values at 312-338 nm and 605-648 nm resulting from electron transition between benzenoid rings (π-π^*) and charge move from benzenoid ring to quinoid ring respectively [28]. The absorption band from 600-700 nm is presumed to be caused by the agglomeration of cerium oxide nanoparticles. The wide band at 480-800 nm is probably the result of the integrated effect of cerium oxide nanoparticles and the transition from the highest occupied energy level to the lowest unoccupied energy level of the quinonoid ring.

The observation of the absorbance peaks of PANI and CeO_2 can be done at different values. For PANI, they can be observed at 356 nm and 635 nm, whereas for CeO_2 they can be observed at 232 nm. 271 nm peaks can be observed for PANI/CeO_2 with different CeO_2 contents for nanocomposites, where the absorbance increases as the ratio of addition to CeO_2 to the polymer increases [29, 30]. As the inorganic contents increase, the intensity of the absorbance increases. Generally speaking, the absorption edge for the nanocomposite is transformed to short wavelengths (high energy) about PANI, which indicates that strong quantum confinement has taken place as a result of hybridization between PANI and CeO_2 material [31].

UV-visible spectroscopy is conducted as a certain interfacial interaction of PANI in the composite has taken place that reveals the fact that the spectrum of PANI containing two prominent peaks at 330–350 nm and 610–680 nm which are associated with the π–π transition of the benzene ring and quinoid ring respectively. The same peak is observed for the composite PANI -$NiCo_2O_4$ with a small shift towards the longer wavelength (red shift). This could be a result of the interfacial interaction between the PANI and $NiCo_2O_4$. This could lead to a strong interaction between PANI and nickel cobaltite, which may have boosted the ion transportation path, to improve the capitative performance [32]. As a result, the absorbance spectra of the prepared samples within a wavelength (210-1000 nm) for PANI/$NiCo_2O_4$/CeO_2 contained peaks referring to the presence of polyaniline, $NiCo_2O_4$ and CeO_2. This indicates the preparation of prepared PANI/$NiCo_2O_4$ /CeO_2.

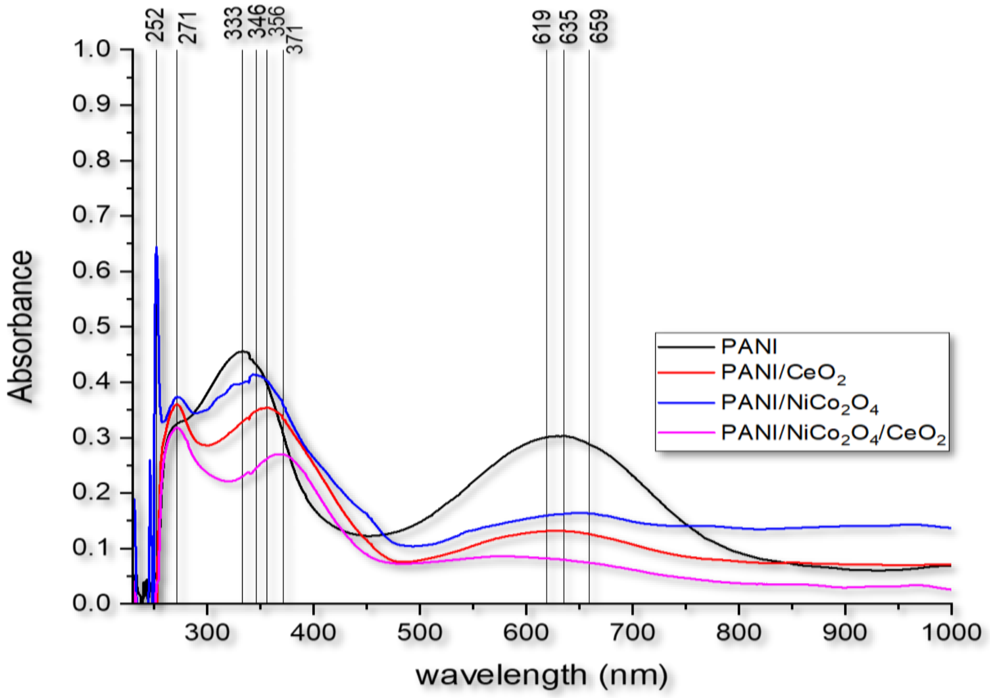

Figure 3. UV–Visible of PANI, PANI/ CeO_2, PANI /$NiCo_2O_4$ and PANI/$NiCo_2O_4$ /CeO_2 nanocomposite

To evaluate the structure and crystallinity of composite materials, XRD analysis is performed. Figure 4 illustrates the XRD patterns of the PANI, PANI/$NiCo_2O_4$, PANI/CeO_2, and PANI/$NiCo_2O_4$/CeO_2. Pristine PANI shows a highly amorphous broad hump from 20 to 35° without demonstrating any sharp crystalline peaks. This shows the highly amorphous nature of PANI. Similar XRD findings are made public elsewhere [33].

A small peak of 25.6° which is associated with PANI is shown by the XRD pattern of PANI/$NiCo_2O_4$ nanocomposite although the XRD peaks of $NiCo_2O_4$ do not show in the XRD pattern of PANI/$NiCo_2O_4$ nanocomposite which is resulted by the deep integration of $NiCo_2O_4$ nanoparticles in PANI matrix. $NiCo_2O_4$ nanoparticles behaved as a template for the growth of PANI during the synthesis. However, sharp and well-defined peaks of CeO_2 in the PANI/CeO_2 nanocomposite. The CeO_2 peaks showed up at 2θ values of 28.6°, 32.9°, 47.4°, 56.3°, 59°, 69.6°, 76.8°, and 79.2°, which are linked to the (111), (200), (220), (311), (222), (400), (311), and (420) crystallographic planes of a cubic fluorite structure of CeO_2 [34, 35].

The peak location of CeO_2 remained of $NiCo_2O_4$ in the PANI/$NiCo_2O_4$/CeO_2, though the intensity of the CeO_2 peaks were significantly reduced. Nevertheless, a broader hump related to PANI is evident, which confirms the successful integration of CeO_2 and $NiCo_2O_4$ nanoparticle in the PANI matrix without showing any impurity phase.

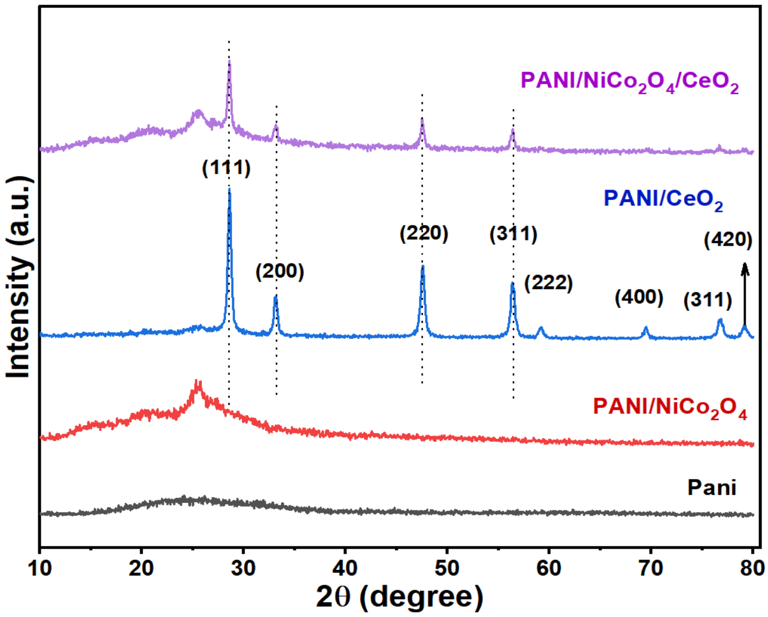

Figure 4. X-ray diffraction patterns of the as-synthesized PANI, PANI/ CeO_2, PANI /$NiCo_2O_4$ and PANI/$NiCo_2O_4$ /CeO_2 nanocomposites

FE-SEM is used to investigate the surface morphology of the prepared composite. FE-SEM images of PANI, PANI/ CeO_2, PANI /$NiCo_2O_4$ and PANI/$NiCo_2O_4$/CeO_2 nanocomposite are illustrated in Figure 5. Figure (5-A) contains the FE-SEM image of pure PANI demonstrating the densely packed tubular shape of PANI. It is well known that the morphology of PANI is tubular while prepared [36].

The PANI morphology did not change upon incorporation of CeO_2 nanoparticles Figure (5-B). On the surface of PANI, a few particles were observed which confirms the fact that $NiCo_2O_4$ nanoparticles were embedded in the PANI tubes Figure (5-C). In the FE-SEM image of PANI/$NiCo_2O_4$ /CeO_2 nanocomposite (Figure 5D), a tubular-shaped PANI with a uniform decoration of CeO_2 and $NiCo_2O_4$ nanoparticles is noticed [37-40]. A more loosely packed PANI tube with a uniform distribution of CeO_2 and $NiCo_2O_4$ nanoparticles can be observed in PANI/$NiCo_2O_4$ /CeO_2 nanocomposite. Figure (5-D) illustrates the production of nanostructures with a minimum size of 18.40 nm.

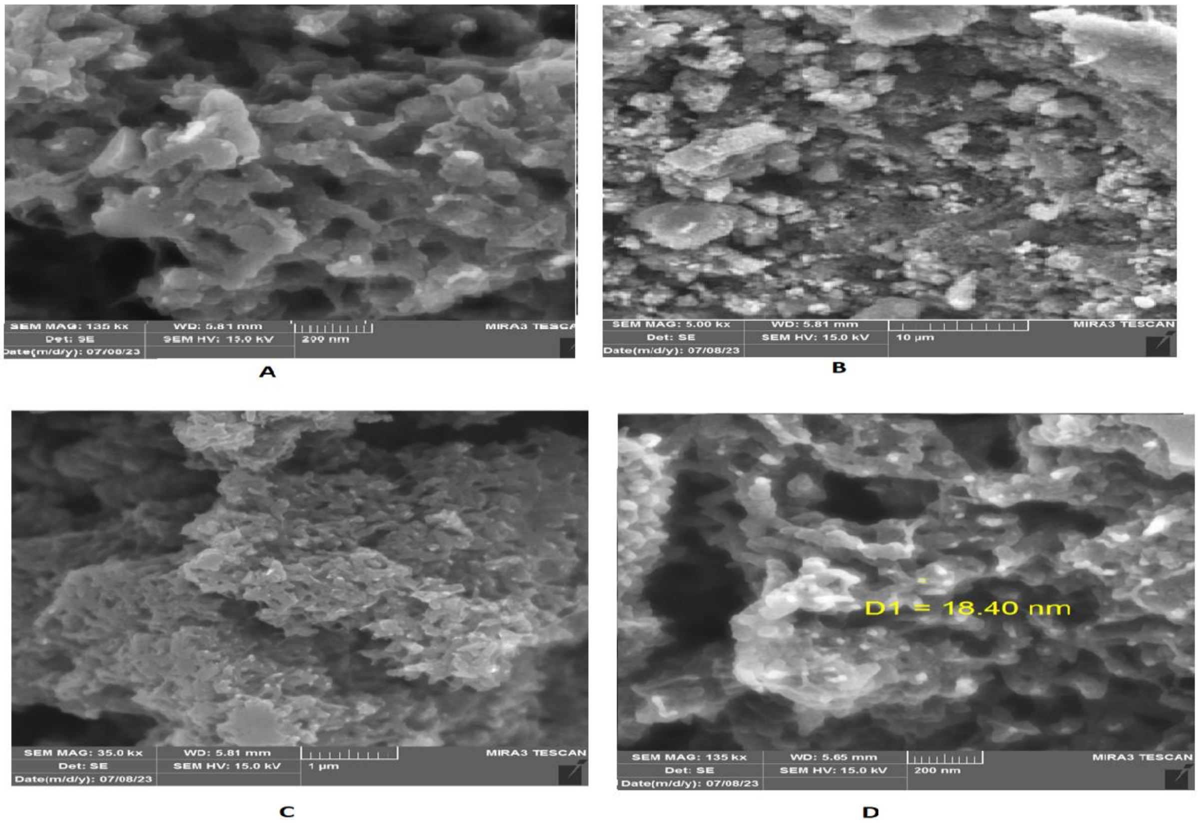

Figure 5. The FE-SEM morphology of the as-synthesized of (A) PANI, (B) PANI/ CeO_2, (C) PANI /$NiCo_2O_4$ and (D) PANI/$NiCo_2O_4$ /CeO_2

Conclusion

To summarize, the innovative PANI/$NiCo_2O_4$/CeO_2 nanocomposite is highly effective, boasting a well-organized, metal-free structure. It has been thoroughly characterized by various studies. The integration of CeO_2 and $NiCo_2O_4$ nanoparticles into the PANI matrix is demonstrated by XRD patterns. The observed blue shift in the UV absorption threshold is due to size quantization effects. FE-SEM has been instrumental in analyzing the morphology and structure of the particles. FT-IR spectra have determined the functional groups in the samples.

REFERENCES

[1] P. M. Ajayan, L. S. Schadler, and P. V. Braun, *Nanocomposite Science and Technology*. John Wiley & Sons, 2006.

[2] X. Du, H.-Y. Liu, G. Cai, Y.-W. Mai, and A. Baji, "Use of Facile Mechanochemical Method to Functionalize Carbon Nanofibers With Nanostructured Polyaniline and Their Electrochemical Capacitance," *Nanoscale Research Letters*, vol. 7, pp. 1-8, 2012.

[3] S. B. Abel, E. I. Yslas, C. R. Rivarola, and C. A. Barbero, "Synthesis of Polyaniline (PANI) and Functionalized Polyaniline (F-PANI) Nanoparticles With Controlled Size by Solvent Displacement Method. Application in Fluorescence Detection and Bacteria Killing by Photothermal Effect," *Nanotechnology*, vol. 29, no. 12, p. 125604, 2018.

[4] H. Xia and Q. Wang, "Ultrasonic Irradiation: A Novel Approach to Prepare Conductive Polyaniline/Nanocrystalline Titanium Oxide Composites," *Chemistry of Materials*, vol. 14, no. 5, pp. 2158-2165, 2002.

[5] J. O. Iroh and K. Levine, "Electrochemical Synthesis of Polypyrrole/Polyimide Conducting Composite Using a Polyamic Acid Precursor," *European Polymer Journal*, vol. 38, no. 8, pp. 1547-1550, 2002.

[6] X. Li et al., "Fabrication of $NiCo_2O_4$@ Polyaniline Heterostructure as Positive Electrode for Asymmetrical Supercapacitor," *Journal of Applied Polymer Science*, vol. 140, no. 43, p. e54580, 2023.

[7] Q. Al-Haidary, A. M. Al-Mokaram, A. H. Ismail, and F. M. Hussein, "State of the Art of Synthesized PANI-(Sn+2/TiO_2) Nanocomposites for Conductive Application," *Al-Mustansiriyah Journal of Science*, vol. 33, no. 1, pp. 32-38, 2022.

[8] N. Jabeen, Q. Xia, M. Yang, and H. Xia, "Unique Core-Shell Nanorod Arrays With Polyaniline Deposited Into Mesoporous $NiCo_2O_4$ Support for High-Performance Supercapacitor Electrodes," *ACS Applied Materials & Interfaces*, vol. 8, no. 9, pp. 6093-6100, 2016.

[9] A. Goel et al., "Synthesis of $NiCo_2O_4$/rGO/PANI Ternary Nanocomposite for Electrochemical Performance and Impact of Doping on Pure PANI," *Journal of Materials Science: Materials in Electronics*, vol. 34, no. 27, p. 1841, 2023.

[10] E. Kumar, P. Selvarajan, and D. Muthuraj, "Preparation and Characterization of Polyaniline/Cerium Dioxide (CeO_2) Nanocomposite via In Situ Polymerization," *Journal of Materials Science*, vol. 47, pp. 7148-7156, 2012.

[11] T. Rajyalakshmi, A. Pasha, S. Khasim, M. Lakshmi, and M. Imran, "Synthesis, Characterization and Hall-Effect Studies of Highly Conductive Polyaniline/Graphene Nanocomposites," *SN Applied Sciences*, vol. 2, pp. 1-11, 2020.

[12] F.-x. Niu, Y.-x. Wang, Y.-t. Zhang, S.-k. Xie, L.-r. Ma, C.-g. Wang, and Y.-p. Mao, "A Hierarchical Architecture of PANI/APTES/SiC Nanocomposites With Tunable Dielectric for Lightweight and Strong Microwave Absorption," *Journal of Materials Science*, vol. 54, pp. 2181-2192, 2019.

[13] C. Pan, Z. Liu, W. Li, Y. Zhuang, Q. Wang, and S. Chen, "$NiCo_2O_4$@ Polyaniline Nanotubes Heterostructure Anchored on Carbon Textiles With Enhanced Electrochemical Performance for Supercapacitor Application," *The Journal of Physical Chemistry C*, vol. 123, no. 42, pp. 25549-25558, 2019.

[14] H. Xu, J.-X. Wu, Y. Chen, J.-L. Zhang, and B.-Q. Zhang, "Facile Synthesis of Polyaniline/$NiCo_2O_4$ Nanocomposites With Enhanced Electrochemical Properties for Supercapacitors," *Ionics*, vol. 21, pp. 2615-2622, 2015.

[15] M. M. Hassen and I. M. Ibrahim, "Synthesis of Polyaniline–Cerium Oxide Nanocomposite for Photodetector Application," *Journal of Physics: Conference Series*, vol. 2114, no. 1, p. 012047, 2021.

[16] A. Al-Kinani, M. Eftekhari, M. Gheibi, and M. Chamsaz, "Polyaniline-Coated Cerium Oxide Nanoparticles as an Efficient Adsorbent for Preconcentration of Ultra-Trace Levels of Cadmium (II) Followed by Electrothermal Atomic Absorption Spectrometry," *Spectroscopy Letters*, vol. 51, no. 6, pp. 287-296, 2018.

[17] D. A. Gopakumar et al., "Cellulose Nanofiber-Based Polyaniline Flexible Papers as Sustainable Microwave Absorbers in the X-Band," *ACS Applied Materials & Interfaces*, vol. 10, no. 23, pp. 20032-20043, 2018.

[18] A. W. A. S. Talluh, R. S. Najm, M. J. Saleh, and J. N. Saleh, "Synthesis, Characterization, and Evaluation of the Biological Activity of Novel Oxazepine Compounds Derived From Indole-5-Carboxylic Acid," *AJBCI*, vol. 1, no. 8, pp. 10-19, Aug. 2024.

[19] A. W. A. S. Talluh, M. J. Saleh, and J. N. Saleh, "Preparation, Characterization and Study of the Molecular Docking of Some Derivatives of the Tetrazole Ring and Evaluation of Their Biological Activity," *WOS*, vol. 1, no. 7, pp. 15-23, Jul. 2024.

[20] A. W. A. S. Talluh, J. N. Saleh, and M. J. Saleh, "Preparation, Characterization and Evaluation of Biological Activity and Study of Molecular Docking of Some New Thiazolidine Derivatives," *Central Asian Journal of Medical and Natural Science*, vol. 5, no. 1, pp. 608-616, 2024.

[21] B. Kuzmanović et al., "The Influence of Oxygen Vacancy Concentration in Nano Dispersed Non-Stoichiometric CeO_2-δ Oxides on the Physicochemical Properties of Conducting Polyaniline/CeO_2 Composites," *Electrochimica Acta*, vol. 306, pp. 506-515, 2019.

[22] A. W. A. S. Talluh, M. J. Saleh, J. N. Saleh, K. Al-Badrany, and H. M. S. Al-Jubori, "Preparation, Characterization, and Evaluation of the Biological Activity of New 2,3-Dihydroquinazoline-4-One Derivatives," *EJMMP*, vol. 4, no. 4, pp. 326-332, May 2024.

[23] M. J. Saleh, J. N. Saleh, and K. Al-Badrany, "Preparation, Characterization, and Evaluation of the Biological Activity of Pyrazoline Derivatives Prepared Using a Solid Base Catalyst," *EJMMP*, vol. 4, no. 7, pp. 25-32, Jul. 2024.

[24] A. W. A. S. Talluh, J. N. Saleh, and M. J. Saleh, "Preparation and Characterization of New Imidazole Derivatives Derived From Hydrazones and Study of Their Biological and Laser Efficacy," *Central Asian Journal of Theoretical and Applied Science*, vol. 5, no. 4, pp. 202-211, 2024.

[25] A. H. Dalaf, M. J. Saleh, and J. N. Saleh, "Green Synthesis, Characterization, and Multifaceted Evaluation of Thiazolidinone Derivatives: A Study on Biological and Laser Efficacy," *EJMMP*, vol. 4, no. 7, pp. 155-168, Jul. 2024.

[26] V. Venkatachalam, A. Alsalme, A. Alghamdi, and R. Jayavel, "Hexagonal-Like $NiCo_2O_4$ Nanostructure Based High-Performance Supercapacitor Electrodes," *Ionics*, vol. 23, pp. 977-984, 2017.

[27] N. V. Nguyen et al., "Facile Synthesis of a $NiCo_2O_4$ Nanoparticles Mesoporous Carbon Composite as Electrode Materials for Supercapacitor," *ChemistrySelect*, vol. 5, no. 23, pp. 7060-7068, 2020.

[28] J. Vidya and P. Balamurugan, "Synthesis, Structural, Morphological, and Optical Characterization of Polyaniline Hydrochloride/Cerium Oxide Nanocomposite," *Materials Today: Proceedings*, vol. 8, pp. 223-230, 2019.

[29] M. Trchová, Z. Morávková, M. Bláha, and J. Stejskal, "Raman Spectroscopy of Polyaniline and Oligoaniline Thin Films," *Electrochimica Acta*, vol. 122, pp. 28-38, 2014.

[30] B. Samai and S. C. Bhattacharya, "Conducting Polymer Supported Cerium Oxide Nanoparticle: Enhanced Photocatalytic Activity for Wastewater Treatment," *Materials Chemistry and Physics*, vol. 220, pp. 171-181, 2018.

[31] R. N. Dhanawade et al., "Highly Sensitive and Selective PAni-CeO_2 Nanohybrid for Detection of NH_3 Biomarker at Room Temperature," *Journal of Materials Science: Materials in Electronics*, vol. 34, no. 9, p. 781, 2023.

[32] M. S. Kumar, K. Y. Yasoda, N. K. Kothurkar, and S. K. Batabyal, "Simple Synthesis Route of Glycine-Assisted PANi-$NiCo_2O_4$ Porous Powder for Electrochemical Application," *Ionics*, vol. 25, pp. 4499-4507, 2019.

[33] A. Bahuguna, P. Choudhary, T. Chhabra, and V. Krishnan, "Ammonia-Doped Polyaniline–Graphitic Carbon Nitride Nanocomposite as a Heterogeneous Green Catalyst for the Synthesis of Indole-Substituted 4H-Chromenes," *ACS Omega*, vol. 3, no. 9, pp. 12163-12178, 2018.

[34] G. Jayakumar, A. A. Irudayaraj, and A. D. Raj, "Particle Size Effect on the Properties of Cerium Oxide (CeO_2) Nanoparticles Synthesized by Hydrothermal Method," *Mechanics, Materials Science & Engineering Journal*, vol. 9, no. 1, 2017.

[35] S. A. A. R. Sayyed, N. I. Beedri, V. S. Kadam, and H. M. Pathan, "Rose Bengal-Sensitized Nanocrystalline Ceria Photoanode for Dye-Sensitized Solar Cell Application," *Bulletin of Materials Science*, vol. 39, pp. 1381-1387, 2016.

[36] Y.-L. Chang, M.-D. Tsai, C.-H. Shen, C.-W. Huang, Y.-C. Wang, and C.-W. Kung, "Cerium-Based Metal-Organic Framework-Conducting Polymer Nanocomposites for Supercapacitors," *Materials Today Sustainability*, vol. 23, p. 100449, 2023.

[37] V. Manikandan, S. Kumar, A. K. Palai, S. Mohanty, and S. Nayak, "Ternary Composite Based on $NiCo_2O_4$/rGO/PANI as an Efficient Pt-Free Tri-Iodide Reducing Agent for Dye-Sensitized Solar Cell Application," *Journal of Photochemistry and Photobiology A: Chemistry*, vol. 382, p. 111939, 2019.

[38] A. W. A. S. Talluh, J. N. Saleh, and M. J. Saleh, "Preparation, Characterization and Evaluation of Biological Activity and Study of Molecular Docking of Some New Thiazolidine Derivatives," *Central Asian Journal of Medical and Natural Science*, vol. 5, no. 1, pp. 608-616, 2024.

[39] A. W. A. S. Talluh, "Preparation, Characterization, Evaluation of Biological Activity, and Study of Molecular Docking of Azetidine Derivatives," *Central Asian Journal of Medical and Natural Science*, vol. 5, no. 1, pp. 608-616, 2024.

[40] A. W. A. S. Talluh, M. J. Saleh, J. N. Saleh, and H. M. S. Al-Jubori, "Synthesis and Characterization of Some New Imine Graphene Derivatives and Evaluation of Their Biological Activity," *Central Asian Journal of Medical and Natural Science*, vol. 5, no. 4, pp. 272-290, 2024.